DOI: 10.1002/chem.201000506

Redox Sorption and Recovery of Silver Ions as Silver Nanocrystals on Poly(aniline-*co*-5-sulfo-2-anisidine) Nanosorbents

Xin-Gui Li,*[a] Hao Feng,[a] and Mei-Rong Huang*[a, b]

Abstract: Poly[aniline(AN)-co-5-sulfo-2-anisidine(SA)] nanograins with rough and porous structure demonstrate ultrastrong adsorption and highly efficient recovery of silver ions. The effects of five key factors—AN/SA ratio, Ag^I concentration, sorption time, ultrasonic treatment, and coexisting ions—on Ag^I adsorbability were optimized, and AN/SA (50/50) copolymer nanograins were found to exhibit much stronger Ag^I adsorption than polyaniline and all other reported sorbents. The maximal Ag^I sorption capacity of up to 2034 mg g^{-1} (18.86 mmol g^{-1}) is the highest thus far and also much higher than the maximal Hg-ion sorption capacity (10.28 mmol g^{-1}). Especially at $\leq$2 mM Ag^I, the nanosorbents exhibit $\geq$99.98% adsorptivity, and thus achieve almost complete Ag^I sorption. The sorption fits the Langmuir isotherm well and follows pseudo-second-order kinetics. Studies by IR, UV/Vis, X-ray diffraction, polarizing microscopy, centrifugation, thermogravimetry, and conductivity techniques showed that Ag^I sorption occurs by a redox mechanism mainly involving reduction of Ag^I to separable silver nanocrystals, chelation between Ag^I and $-NH-/-N=/-NH_2/-SO_3H/-OCH_3$, and ion exchange between Ag^I and H^+ on $-SO_3^-H^+$. Competitive sorption of Ag^I with coexisting Hg, Pb, Cu, Fe, Al, K, and Na ions was systematically investigated. In particular, the copolymer nanoparticles bearing many functional groups on their rough and porous surface can be directly used to recover and separate precious silver nanocrystals from practical Ag^I wastewaters containing Fe, Al, K, and Na ions from Kodak Studio. The nanograins have great application potential in the noble metals industry, resource reuse, wastewater treatment, and functional hybrid nanocomposites.

Keywords: copolymers · macromolecular chemistry · nanoparticles · redox chemistry · silver

Introduction

Silver is a precious metal used worldwide as currency and in functional nanomaterials for antimicrobial activity,[1] DNA and microRNA detection,[2] multicolor photochromism,[3] color luminescence,[4,5] self-erasing multicolor imaging,[6] catalytic activity, and optoelectronic effects.[7] Compared with early inefficient methods, modern techniques for silver recovery from scrap and wastewaters such as photographic films, X-ray films, and jewelry are highly efficient, and include sorption, precipitation, ion exchange, reductive exchange, and electrolysis. Some modern sorbents, such as polymers,[8–11] chitosan,[12–13] carbonaceous materials,[14] coal,[15] and layered sulfides,[16] have already exhibited very good performance for recovery of noble and heavy metals. Among them, aromatic amine polymers synthesized by chemical oxidative polymerization have various important technological applications, such as sorbents, rechargeable batteries, electrocatalysts, microelectronic and electrochromic devices, smart windows, sensors, and actuators, due to their unique multifunctionality, including excellent redox reversibility, variable conductivity, strong electroactivity, colorful electrochromism, and high environmental stability.[17–19] Recent studies on aromatic amine polymers revealed their tremendous application potential for the removal and recovery of heavy-metal ions from aqueous solution,[20–23] because of the many functional groups such as $-NH-$, $-N=$, and $-NH_2$ directly linked to the benzenoid and quinoid units which can reversibly adsorb and complex metal ions. Furthermore, a greater number of various functional groups would presumably result in stronger adsorption, higher reac-

[a] Prof. Dr. X.-G. Li, H. Feng, Prof. M.-R. Huang
Institute of Materials Chemistry
Key Laboratory of Advanced Civil Engineering Materials
College of Materials Science & Engineering, Tongji University
1239 Si-Ping Road, Shanghai 200092 (China)
Fax: (+86) 21-65980524
E-mail: adamxgli@yahoo.com

[b] Prof. M.-R. Huang
Key Laboratory of Molecular Engineering of Polymers
Fudan University, Shanghai 200433 (China)
E-mail: meironghuang@ymail.com

tivity, and better complexation of metal ions. However, there have been no systematic investigations on the adsorbability of Ag^I ions, especially from practical wastewater onto aromatic amine polymers containing more functional groups. Highly reactive sorption and recovery of silver ions from the practical wastewater containing a variety of metal ions onto polymer nanosorbents remain a considerable challenge.

To further increase the amount of functional groups and thus greatly enhance the adsorbability and recoverability of heavy-metal ions, aniline (AN) and 5-sulfo-2-methoxyaniline (SA) were chosen for facile synthesis of fine AN/SA copolymer nanograins[21] as novel nanosorbents by chemical oxidative polymerization. It has been reported that copolymer nanograins having even more functional groups, including sulfo, methoxyl, −NH−, −N=, and $-NH_2$ groups are excellent nanosorbents for a highly efficient removal of Hg^{II} from aqueous solution,[21] because introduction of sulfo and methoxyl groups having intrinsic static repulsion and electron-donating ability is very beneficial to the formation, dispersion, and self-stability of aniline copolymer nanoparticles, and thus to functional-group exposure and to reactive sorption of heavy-metal ions on the nanoparticle surface. Therefore, it could be speculated that Ag^I, which has high oxidation ability, would be reactively adsorbed as Ag nanocrystals onto the copolymer nanograins, and thus highly effective recovery of silver from industrial wastewater and in daily life would be achieved. The copolymer nanograins may be a cost-effective nanosorbent for the efficient purification and recovery of heavy-metal ions including Ag^I ions, and may also allow facile fabrication of functional hybrid nanocomposites consisting of copolymer nanograins and Ag nanocrystals.

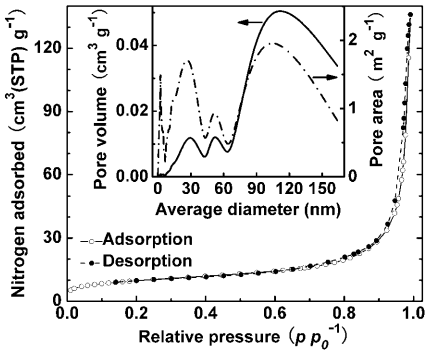

Figure 1. Nitrogen adsorption/desorption isotherm plots of dry AN/SA (50/50) copolymer particles. The pore distribution curves are shown in the inset.

Results and Discussion

Optimization of AN/SA ratio for Ag^I sorption onto copolymer nanograins: The chemical oxidative polymerization of AN and SA comonomers in HCl simply and directly affords fine, uniform, and black AN/SA (50/50) copolymer nanograins having the following physical characteristics:

1) Specific surface area: 35.22 $m^2 g^{-1}$ (Figure 1).
2) Pore size: 28.16 nm.
3) Pore volume: 0.21 $cm^3 g^{-1}$.
4) Apparent density: 0.247 $g cm^{-3}$.
5) Bulk density: 0.313 $g cm^{-3}$.
6) Number-average diameter: approximately 82.2 nm by laser particle size analysis.
7) Morphology: a diameter of about 51 nm (ca. 30 nm without Au layer) and a length of 170–450 nm (ca. 150–430 nm without Au layer) by FE-SEM (Figure 2).
8) Bulk electrical conductivity: 0.0463 $S cm^{-1}$.

After introduction of methoxyl and sulfo groups into the polyaniline, not only were as-prepared AN/SA (50/50) copolymer nanograins with a rough and porous morphology obtained, but also their adsorption capability toward Ag^I rose significantly, and reached a maximum at the feed AN/SA molar ratio of 50/50 (Figure 3). The maximal sorption capacity (269.1 $mg g^{-1}$) of Ag^I onto the AN/SA (50/50) copolymer nanograins is 21% higher than that of 219.7 $mg g^{-1}$ onto polyaniline microparticles under the same conditions. Polyaniline microparticles have strong Ag^I adsorption/reducibility, but the AN/SA (50/50) copolymer nanograins have even stronger Ag^I adsorption capability/reducibility, indicating that the nanograins are powerful Ag^I nanosorbents and hybrid Ag nanocrystal/copolymer nanograin nanocomposites with potential application as electrode modifiers due to their high catalytic activity.[7] Apparently, this significantly

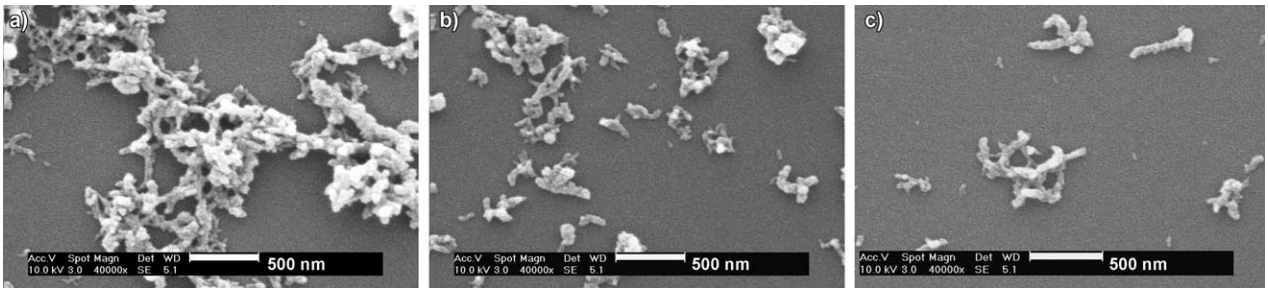

Figure 2. FE-SEM images of AN/SA (50/50) copolymer nanograins synthesized with a comonomer/oxidant molar ratio of 1/1 in 1.0 M HCl at 25 °C for 24 h.

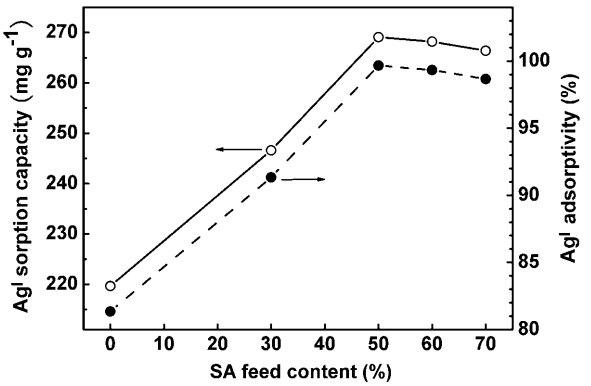

Figure 3. Variation of the sorption capacity and adsorptivity of Ag^I onto 50 mg of AN/SA copolymer nanograins with SA feed content at an initial Ag^I concentration of 5 mM in 25 mL $AgNO_3$ solution at 30 °C for 48 h.

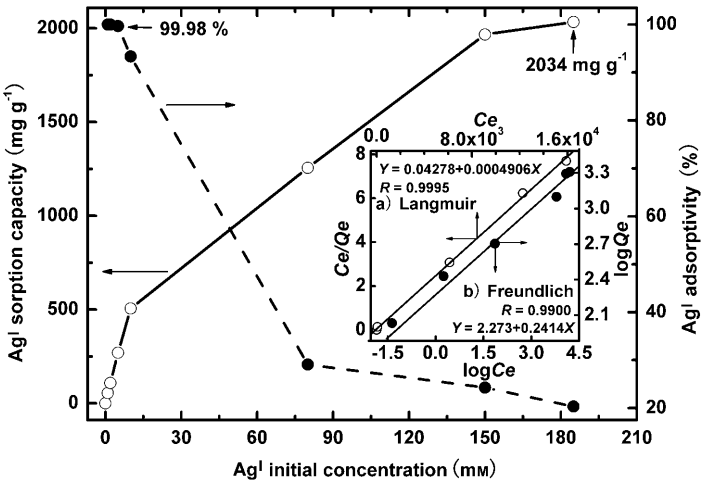

Figure 4. Effect of initial Ag^I concentration on Ag^I sorption onto 50 mg of AN/SA (50/50) copolymer nanograins in 25 mL $AgNO_3$ solution at 30 °C for a sorption time of 72 h at an initial Ag^I concentration $\leqq 10$ mM and 120 h at an initial Ag^I concentration of >10 mM. Inset: a) Langmuir and b) Freundlich isotherm models for Ag^I sorption.

improved adsorbability is attributable to the rough-surface nanostructures, on which the methoxyl and sulfo groups containing oxygen and sulfur atoms offer more lone-pair electrons that can spontaneously attract electron-poor heavy-metal ions. Notably, the water solubility of the nanograins gradually becomes stronger at a feed SA content higher than 50 mol% because of their inherent hydrophilicity due to more sulfo groups, which consequently leads to slightly reduced adsorbability. Therefore, the copolymer with higher than 50 mol% SA feed content is not a suitable sorbent for the elimination and recovery of heavy-metal ions from aqueous solution. It can be concluded that the AN/SA (50/50) copolymer nanograins are an optimal nanosorbent for the removal and recovery of Ag^I ions from aqueous solutions. The AN/SA (50/50) copolymer nanograins were used in all of the following studies.

Reactive sorption of Ag^I onto AN/SA (50/50) copolymer nanograins

Effect of initial Ag^I concentration and sorption isotherm: As shown in Figure 4, at a very low initial Ag^I concentration of ≤ 2 mM, the copolymer particulate nanosorbents exhibit 99.98% adsorptivity, that is, almost 100% of Ag^I ions can be completely adsorbed and recovered by the nanosorbents. Although the Ag^I adsorptivity decreases from 99.98 to 20.36% with increasing initial Ag^I concentration from 1 to 185 mM, the Ag^I sorption capacity steadily rises from 53.99 to 2034 mg g^{-1}. A similar dependency of the adsorbability on the initial Ag^I concentration was observed when poly(1,8-diaminonaphthalene)[22] and 4-sulfodiphenylamine/1,8-diaminonaphthalene copolymer[23] microparticles were used as sorbents. These results suggest that the AN/SA (50/50) copolymer nanograins not only completely eliminate and recover trace amounts of silver ions, but also most efficiently recover Ag^I ions at high concentration, that is, the copolymer nanograins with the highest experimental Ag^I sorption capacity of 2034 mg g^{-1} (18.86 mmol g^{-1}) are the most powerful silver-ion sorbents known until now, because their adsorbability is even higher than those of silver ions onto poly(1,8-diaminonaphthalene)[22] and 4-sulfodiphenylamine/1,8-diaminonaphthalene copolymer[23] under similar sorption conditions. In particular, the experimental Ag^I sorption capacity of 18.86 mmol g^{-1} is much higher than the experimental $Hg^{I\&II}$ sorption capacity of 10.28 mmol g^{-1} onto the same nanosorbents.[21] Thus, the AN/SA (50/50) copolymer nanograins are very strong mercury-ion and ultrastrong Ag^I nanosorbents.

Linearized Langmuir and Freundlich isotherm sorption models were applied to quantitatively analyze the sorption equilibrium of Ag^I onto the nanograins (Figure 4 and Table 1). It appears that both models can well describe the sorption, whereby the Langmuir model has a higher correlation coefficient and smaller standard deviation. The theoretical maximum sorption capacity Q_m determined by the Langmuir isotherm gives a total capacity for Ag^I of 2038 mg g^{-1}, which is very consistent with the experimental maximum adsorbance of 2034 mg g^{-1}.

Comparison of Ag^I adsorbability with other sorbents: Since the different sorption conditions used by different investiga-

Table 1. Isothermal models for Ag^I sorption onto AN/SA copolymer nanograins.[a]

Model	Model equations	Correlation coefficient	Standard deviation	Q_m [mg g^{-1}] or n	K_a [L mg^{-1}] or K_F
Langmuir	$C_e/Q_e=(C_e/Q_m)+1/K_aQ_m$	0.9995	0.01142	$Q_m=2038$	$K_a=0.01147$
Freundlich	$\lg Q_e=[(1/n)\lg C_e]+\lg K_F$	0.9900	0.09614	$n=4.14$	$K_F=187.3$

[a] Q_m: sorption capacity at saturation, n: sorption equilibrium constant, K_a: sorption coefficient, K_F: equilibrium constant indicating sorption capacity.

Table 2. Comparison of Ag^I adsorbability between AN/SA (50/50) copolymer nanograins and other sorbents.

Sorbents name	dosage [mg]	Initial Ag^I solution c [mM]	pH	Ag^I+Ag^0 sorption capacity [mg g^{-1}]	adsorptivity [%]	Ag^0 Obtained [mg g^{-1}]	Recovery [%]	Q_m by Langmuir model	Rate constant k [h^{-1}] or sorption time t [h]	Refs.
poly(*o*-phenylenediamine)	50	100	5.4	540	10	400	7.4	285	$k=0.119$	[20]
poly(1,8-diaminonaphthalene)	50	82	5.3	819	18.5	574	13.0	885	$k=0.19$	[22]
poly(4-sulfonic diphenylamine-co-1,8-diaminonaphthalene)	50	84	5.3	1144	25.3	996	22.0	1879	$k=0.60$	[23]
AN/SA (50/50) copolymer nanograins	50	80	5.5	1256	29.1	1192	27.6	2038	$k=0.041$	this work
		10	6.5	506	93.3	500	92.4			
bis-thiourea–formaldehyde resin	100	10	6.5	745	68.9	0	0	918	$k=0.22$	[10]
electrooxidized carbon fiber	40	5	10.5	399.6	59.2	396	58.6	437.4	$t=24$	[11]
carbonaceous from flax shives	19	5	5.0	225	32.4	201	32.4	230	$k=0.0177$	[13]
activated carbon	5000	0.46	6.0	0.734	0.91	very few	–	0.734	$t=72$	[14]
coke	5000	0.46	6.0	3.06	3.83	very few	–	3.06	$t=72$	[14]
bituminous coal	5000	0.46	6.0	1.0–40.9	1.24–51.1	very few	–	1.0-40.9	$t=72$	[14]
Shenfu3^{-1} coal	50	60	6.5	86.5	66.7	very few	–	107	$k=1.26$	[15]
brewery waste biomass	100	1	4.0	42.8	79.3	very few	–	42.8	$t=3$	[25]

tors may cause differences in Ag^I adsorbability, a detailed comparison between AN/SA (50/50) copolymer nanosorbents and other sorbents is listed in Table 2. Obviously, the copolymer nanosorbents have stronger adsorbability than any other sorbents despite the initial Ag^I concentration, because the nanosorbents possess very high experimental Q_e and theoretical Q_m. The copolymer nanosorbents have even stronger adsorbability than poly(4-sulfodiphenylamine-co-1,8-diaminonaphthalene) microsorbents containing more $-NH_2$ and $-NH-$ groups,[23] because the nanosorbents have much higher specific surface area and porosity. Moreover, the copolymer nanosorbents have higher Ag metal recovery than any other sorbents under similar sorption conditions. In other words, 94.9 [$=(1192\div1256)\times100\,\%$] to 98.8 % [$=(500\div506)\times100\,\%$] of the Ag^I adsorbed onto the copolymer is reduced to Ag metal on sorption. Although some other traditional sorbents like bis-thiourea–formaldehyde resin, brewery waste biomass, and Shenfu3^{-1} coal are good for sewage disposal, they may be unsuitable for efficient recovery of precious metals because the metal ions are only transferred from liquid phase to solid phase without valence change. To effectively acquire precious elemental metals, further treatment must be implemented when traditional sorbents are used. One exception is the slower sorption of the copolymer nanosorbents compared to some other sorbents such as Shenfu3^{-1} coal, oxidative aromatic diamine polymers, and bis-thiourea–formaldehyde resin, which indicates that the copolymer nanosorbents have long-lasting reducing action towards Ag^I ions because of their unique sorption mechanism, which is discussed in detail below.

Effect of sorption time and sorption kinetics: Figure 5 a shows the Ag^I sorption capacity and adsorptivity profiles versus sorption time on the AN/SA (50/50) copolymer nanograins. The sorption capacity and adsorptivity of Ag^I on the nanograins both increase nonlinearly with sorption time. The sorption process includes two stages: a secondary but instant stage and a primary but gradual stage. The faster

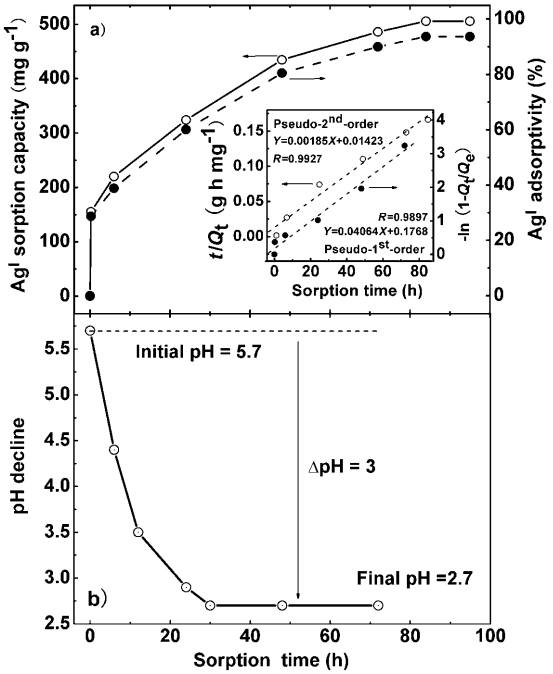

Figure 5. Effect of sorption time on a) Ag^I sorption onto 50 mg of AN/SA (50/50) copolymer nanograins at an initial Ag^I concentration of 10 mM and b) pH value of Ag^+ sorption solution in the presence of 50 mg of AN/SA (50/50) copolymer nanograins at an initial Ag^+ concentration of 2 mM in 25 mL of $AgNO_3$ solution at 30 °C.

step may be attributed to physical surface sorption of Ag^I onto the high surface energy nanoparticles, while the slower step may represent redox, chelation, and ion-exchange interactions between Ag^I and five types of functional groups of the nanoparticles over a long period.

To investigate the mechanism of sorption, two kinetic models are generally used to test experiment data. It can be concluded from Figure 5 a (inset) that the sorption process accords well with the pseudo-second-order model with a higher correlation coefficient of 0.9927 than with the

pseudo-first-order model with a correlation coefficient of 0.9897. The pseudo-second-order model is based on the assumption that the chemical sorption behavior between adsorbent and adsorbate over the whole range of sorption mechanism is a rate-controlling step,[25] which means that the sorption mechanism of Ag^{I} on the grainy nanosorbents is chemically reactive sorption including redox, chelation, and ion exchange.

Effect of ultrasonic treatment of the copolymer nanograins: Since the nanograins with rough and porous morphology and thus high surface energy are prone to aggregate during the drying process, ultrasonic treatment before sorption is necessary to make sure that they are completely dispersed into fine nanograins. This treatment allows some inner functional groups to be exploited effectively. The effect of ultrasonic treatment on Ag^{I} sorption of the copolymer nanograins is shown in Figure 6.

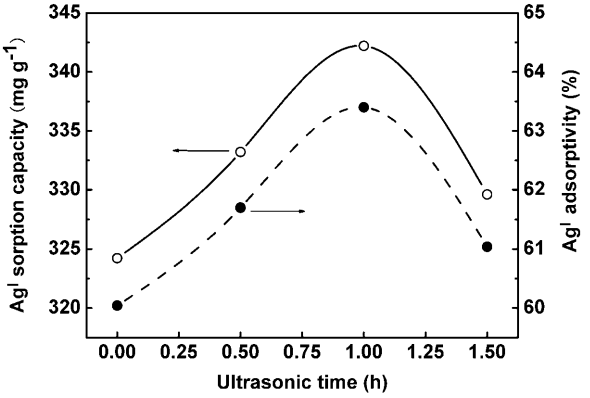

Figure 6. Effect of ultrasonic pretreatment of the AN/SA (50/50) copolymer nanograins in distilled water on the sorption of Ag^{I} onto 50 mg of copolymer nanograins at an initial Ag^{I} concentration of 10 mM in 25 mL of $AgNO_3$ solution at 30 °C for 24 h.

The sorption capacity and adsorptivity of Ag^{I} ions both increase during the first treatment time of 1 h, and then decrease with a further increases in ultrasonication time up to 1.5 h. Ultrasonic treatment can strongly disperse the aggregated particles from each other, as was proved by particle size analysis.[21] With increasing ultrasonication time from 0 to 1 h, the number-average diameter monotonically decreases from 3.42 μm to 120 nm, while the size polydispersity index also decreases slightly from 1.26 to 1.12.[21] As a result, Ag^{I} ions can more easily enter into the inside of the nanograins and interact with the inner functional groups. Accordingly, Ag^{I} sorption capacity increases by 5.50% and adsorptivity by 5.67%. However, ultrasound has tremendous energy, and thus can destroy the structure of copolymer macromolecules to some extent, including elimination of functional groups and the rupture of copolymer main chains, and hence adsorbability decreases when ultrasonication time is increased from 1 to 1.5 h. Thus, ultrasonic frequency and time should be chosen to efficiently disperse the copolymer particles without damaging their molecular structure.

Effect of coexisting ions in Ag^{I} solution: Generally, coexisting ions in Ag^{I} solution would severely affect the sorption ability of the target Ag^{I} ions. The powerful adsorbability of Hg^{II} ions onto AN/SA copolymer nanograins was demonstrated previously.[21] Accordingly, we first took Hg^{II} as competitive ion to examine the Ag^{I} sorption stability, which is one of the important factors for fully evaluating nanosorbents. Surprisingly, the Hg^{II} ions only slightly interfere with Ag^{I} sorption onto the copolymer nanosorbents. As summarized in Table 3, even if the initial Hg^{II} concentration is increased up to 400 mg L^{-1}, that is, twice the Ag^{I} concentration, the Ag^{I} adsorptivity decreases only slightly from 99.9% to 93.6%, whereas the Hg^{II} adsorptivity remains nearly constant at 96.5–96.4%. The Hg^{II} adsorptivity of 96.5–96.4% is only slightly lower than the pure Hg^{II} adsorptivity of 99.6–99.9% in the absence of Ag^{I} ions, that is, the Ag^{I} and Hg^{II} ions only slightly interfere with each other. This proves that the copolymer nanograins demonstrate not only outstanding Ag^{I} recovery regardless of the coexistence of Hg^{II} ions, but also great potential for removal of the other heavy-metal ions from heavily polluted wastewater at the same time. Therefore, competitive adsorption among Ag^{I}, Pb^{II}, and Cu^{II} ions was carried out to further confirm this capability. Since heavy-metal ions are highly toxic to human and animal organisms even at very low concentration, a mixed solution with initial $Ag^{I}/Pb^{II}/Cu^{II}$ concentration of 50/50/50 mg L^{-1} was used for the competitive adsorption study. As expected, the copolymer nanograins exhibit comprehensive adsorbability towards a variety of heavy-metal ions even at low concentration (Table 4). The powerful adsorbability of Ag^{I} and Hg^{II} onto the copolymer nanograins, together with good adsorbability of Pb^{II} and Cu^{II},

Table 3. Effect of coexisting Hg^{II} ions on Ag^{I} recovery on 50 mg of AN/SA (50/50) copolymer nanograins in 25 mL of solution at 30 °C for 6 h.

Ag^{I} initial concentration [mg L^{-1}]	Hg^{II}	Ag^{I} concentration after sorption [mg L^{-1}]	adsorptivity [%]	Hg^{II} concentration after sorption [mg L^{-1}]	adsorptivity [%]	Conductivity of the copolymer adsorbing Ag^{I}&Hg^{II} [S cm^{-1}]
0	0	–	–	–	–	0.0463
200	0	0.216	99.9	0	–	0.0748
200	200	2.576	98.8	7.105	96.5	0.4087
200	400	12.78	93.6	14.32	96.4	2.22
0	200	–	–	0.221	99.9	–
0	400	–	–	1.60	99.6	–

Table 4. Effect of coexisting Pb^{II} and Cu^{II} ions on Ag^{I} adsorbability onto 50 mg of AN/SA (50/50) copolymer nanograins in 25 mL of solution at 30 °C for 6 h.

Co-existing ions	Ion concentration [mg L^{-1}] before sorption	after sorption	Ion adsorptivity [%]
Ag^{I}	50	0.0301	99.9
Pb^{II}	50	8.634	82.7
Cu^{II}	50	15.72	68.6

should be mainly attributable to the soft acid groups $-SO_3H$, $-OCH_3$, $-NH_2$, $-NH-$, and $-N=$ in the copolymer chains spread over the rough surface of the nanograins, that interact more easily with soft metal ions such as Ag^{I} and Hg^{II} than with other heavy-metal ions.

Elucidation of sorption mechanism: Generally, metal ions are adsorbed on traditional sorbents by three adsorption mechanisms: surface adsorption, ion exchange and complex sorption. Because AN/SA copolymer nanograins with rough surface and high surface energy were used as sorbent, surface physical sorption of the Ag^{I} onto the nanograins must occur through weak van der Waals force between the nanograins as sorbent and Ag^{I} as adsorbate, but this weak van der Waals interaction is not stable, and the adsorbates can easily fall off of the sorbents. An ion-exchange sorption mechanism also exists through ion exchange between Ag^{I} and active protons on the sulfo groups, which are the main functional groups in the most ion-exchange resins, and this was verified by the decline in pH of the Ag^{I} solution after the sorption process, because the H^{+} replaced by Ag^{I} was released into the solution (see Scheme 1, Figure 5b, and Table 5).

According to the theory of hard and soft acids and bases, soft metal ions such as Ag^{I}, Au^{III}, and Hg^{II} tend to form stable chelates with N-, O- and S-containing functional groups including $-NH_2$, $-NH-$, $-N=$, $-CN$, $-OCH_3$, $-SO_3H$, $-SR$, and $-SH$. The amino and imino groups on the polyaniline chains have strong chelating ability with various metal ions,[20–23] and chelation sorption is one of the most important sorption mechanisms. Such chelation sorption between AN/SA copolymer nanograins and Ag^{I} ions is depicted in Scheme 1. Ion-exchange sorption and chelation sorption are more stable than surface sorption for most sorbents. The ion-exchange process is reversible and significantly influenced by pH and other sorption conditions. As a result, chelation sorption is even more stable than ion-exchange sorption.

Moreover, redox sorption generally occurs if heavy-metal ions like Ag^{I} and Hg^{II} having a certain oxidizability meet the polymers having a certain reducibility in aqueous dispersion.[20–23,27] Such redox sorption does indeed occur during the sorption of Ag^{I} and Hg^{II} ions with a high standard reduction potential, whereby the AN/SA copolymer particles act as a reductant and the Ag^{I} and Hg^{II} ions as an oxidant. During the sorption process, the $-NH_2/-NH-$ groups and benzenoid rings of the AN/SA copolymer chains are oxidized to $-N=$ groups and quinoid rings, respectively, accompanied by reduction of Ag^{I} and Hg^{II} ions to Ag and Hg metals. Therefore, evidence for the redox sorption mechanism of Ag^{I} onto the copolymer nanograins was obtained as follows.

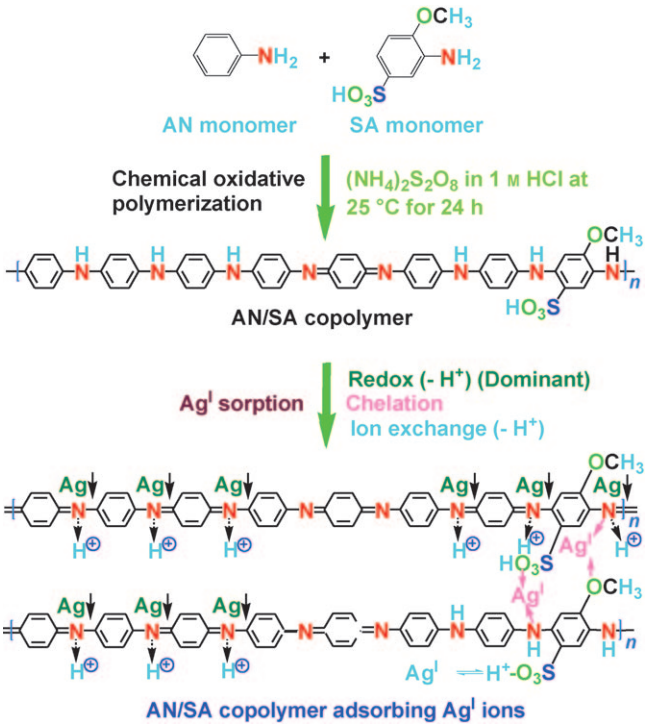

Scheme 1. Nominal copolymerization of aniline (AN) and 5-sulfonic-2-anisidine (SA) and possible reactive sorption mechanism of silver ions onto the AN/SA copolymer nanograins.

Table 5. Adsorptivity of Ag^{I} and other metal ions in genuine 25 mL of Ag^{I}-containing wastewater at 25 °C on 50 mg AN/SA (50/50) copolymer nanograins for 120 h.

Main metal ions	Ion concentration [mg L^{-1}] before sorption	after sorption	Ion adsorptivity [%]	pH decline after sorption ΔpH
Ag^{I}	2060	166	91.9	
Fe^{III} & Fe^{II}	3090	1740	43.7	
Na^{I}	1970	1270	35.5	4.7−5.5 = −0.8
Al^{III}	14.0	10.0	28.6	
K^{I}	650	590	9.2	

Evidence from pH decline of the sorption solution: A monotonic pH decline of the Ag^{I} solution was found with increasing sorption time from 0 to 8 h (Figure 5b), because the H^{+} ions on the sulfo groups of the copolymer particles were gradually replaced by Ag^{I} ions and then released into solution. Apparently, the ion-exchange mechanism plays an important role in the sorption process of Ag^{I} onto the copolymer particles. However, a contradiction was found between calculated and the experimental concentrations of H^{+}. Drastic decline of the solution pH suggests that many more H^{+}

ions were transferred to solution than anticipated. Accordingly, another overwhelming sorption mechanism (i.e., redox sorption) must be operative during the sorption process of Ag^I onto the copolymer particles.

Evidence from IR spectra: The IR spectra of the AN/SA (50/50) copolymer nanograins before and after Ag^I sorption are presented in Figure 7. A broad medium-intensity peak

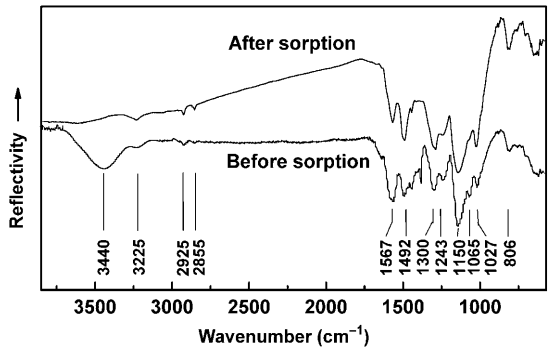

Figure 7. IR spectra of AN/SA (50/50) copolymer nanograins before and after adsorbing 25 mL 80 mM $AgNO_3$ solution at 30 °C for 120 h.

centered at 3440 cm^{-1} due to the characteristic stretching vibration of N–H bonds of $-NH_2$ and –NH– groups in the copolymers tremendously declines or even disappears on Ag^I sorption. The significantly decreased amounts of $-NH_2$ and –NH– groups suggest they are almost completely oxidized to =N– groups by Ag^I. Notably, the IR spectra of copolymer particles adsorbing mercury ions in 25 mL of 10.05 mM $Hg(NO_3)_2$ solution for 48 h still show a broad moderate-intensity peak at 3440 cm^{-1},[21] because much lower Hg^{II} concentration and much shorter sorption time than 80 mM $AgNO_3$ solution for 120 h can only oxidize a small amount of $-NH_2$ and –NH– groups to =N– groups. Weak absorption peaks at 3225 and 2925/2855 cm^{-1} due to the characteristic stretching vibration of respective aromatic C–H and asymmetric/symmetric C–H stretching vibrations in $-OCH_3$ hardly change on Ag^I sorption, that is, the aromatic rings and $-OCH_3$ were not broken by the Ag^I ions as oxidant during the sorption process. The peaks at 1567 and 1492 cm^{-1} are assigned to the characteristic stretching vibrations of quinoid and benzenoid rings, respectively. The peaks at 1300 and 1243/1065 cm^{-1} are associated with the C=N stretching vibration in quinoid rings and C–N stretching vibration in benzenoid rings, respectively. The peak at 1300 cm^{-1} becomes stronger but the peak at 1065 cm^{-1} weaker upon Ag^I sorption, indicative of dehydrogenation and oxidation of C–NH– in the polymer chains to C=N. At the same time, these IR spectral changes give indirect evidence of Ag^I reduction to Ag^0. The three peaks at 1150/1027 and 806 cm^{-1} that are related to the asymmetric/symmetric stretching vibrations of the S=O group in $-SO_3^-$ and 1,2,4,5-tetrasubstituted benzenoid ring of SA units, respectively, hardly vary with Ag^I sorption, which implies that only AN units are oxidized by Ag^I, in good agreement with Hg^{II} sorption onto the same nanograins.[21] A gradual upward trend of the IR spectrum at lower wavenumber of the nanograins adsorbing Ag^I could be a further evidence for oxidation of the conducting nanograins by Ag^I ions, and this is also in accordance with the IR spectra of the nanograins oxidized by Hg^{II} ions.[21]

Evidence from UV/Vis spectra: UV/Vis spectra of the AN/SA (50/50) copolymer particles before and after Ag^I sorption are shown in Figure 8. Under the precondition of con-

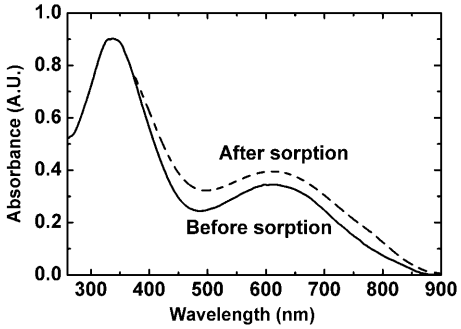

Figure 8. UV/Vis spectra of AN/SA (50/50) copolymer particles adsorbing 25 mL of 80 mM $AgNO_3$ solution at 30 °C for 120 h.

stant band intensity at 338 nm due to π–π* transition, the band at 611 nm due to n–π* transition, which reflects the large π-conjugated structure of the copolymer chains, becomes stronger and slightly redshifted on Ag^I sorption,[28] which is consistent with a previous study on Hg^{II} sorption.[21] Thus, the copolymer nanograins were oxidized by Ag^I and doped with very fine Ag nanocrystals that are the product of the redox interaction between the copolymer nanograins and Ag^I ions.[29,30] The UV/Vis analysis is consistent with the IR results, and further supports the redox sorption mechanism of Ag^I onto the nanograins.

Evidence from wide-angle X-ray diffraction: The crystalline structure of the AN/SA (50/50) copolymer particles before and after Ag^I sorption was characterized by wide-angle X-ray diffraction (Figure 9). Compared with amorphous copolymer nanograins, the Ag-loaded particles exhibit three very sharp diffraction peaks at Bragg angles of 38.1, 44.6, and 64.7°, which exactly correspond to the (111), (200), and (220) crystal planes of Ag metal, respectively. This means that the Ag^I ions were reduced to Ag nanocrystals by the copolymer nanograins during sorption. In particular, the relative intensity of the three diffraction peaks compared with the diffraction intensity of the copolymer particles at a Bragg angle of around 23° becomes increasingly stronger with increasing Ag^I sorption time from 0.5 to 120 h or Ag^I concentration from 10 to 19 mM, that is, more and more Ag nanocrystals are formed and deposited on or doped into the copolymer nanograins.

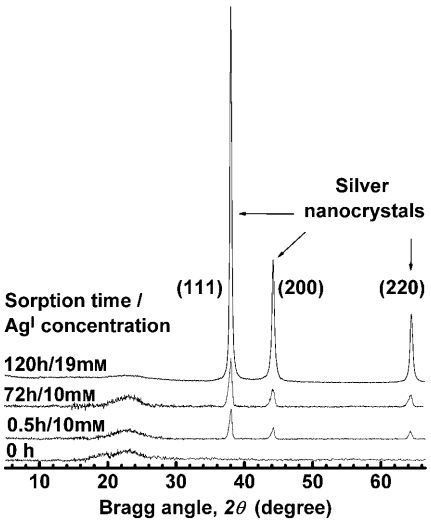

Figure 9. Wide-angle X-ray diffraction curves of AN/SA (50/50) copolymer nanograins adsorbing silver ions from 10 mM Ag^{I} solution and actual 19.1 mM Ag^{I} wastewater.

Evidence from cross-polarizing microscopy: Considering that a great difference between the crystalline ordered structures of Ag nanocrystals and the non-crystalline copolymer nanograins revealed by X-ray diffraction in Figure 9, cross-polarizing microscopy is more suitable to observe the ordered Ag nanocrystals in the amorphous unordered copolymer nanograins than scanning and transmission electron microscopy.[20] As shown in Figure 10, compared with wholly black view of the pure nanograins without adsorbing Ag^{I} ions, the views of the Ag-loaded nanograins become brighter with increasing Ag^{I} concentration or sorption time. Apparently, the bright points and zones imply the presence of anisotropically ordered Ag nanocrystals and their thin aggregates in the almost optically isotropic nanograins because, although the Ag reduced by the copolymer nanograins is in the form of anisotropically ordered crystals,[20] the crystals would not transmit the cross-polarized light if their size and thickness were much larger than 100 nm. In short, more Ag nanocrystals are formed at higher Ag^{I} concentration or longer sorption time, in agreement with the result obtained by X-ray diffraction.

Evidence from centrifugation: Considering the large density difference between the AN/SA copolymer nanograins and Ag nanocrystals, centrifugal separation was employed to macroscopically verify the presence of much heavier Ag nanocrystals in the much lighter copolymer nanograins. Lustrous silver-gray crystals (5.3 mg) were indeed separated from the nanoparticle sorbent after centrifugal treatment for 10 min at 3000 rpm. If all the Ag^{I} ions in 25 mL 2 mM $AgNO_3$ solution were adsorbed onto the copolymer nanograins and simultaneously reduced to Ag^{0}, there should have been 5.4 mg of Ag nanocrystals in the final copolymer nanograins. Therefore, it is concluded that 98.1% of the Ag^{I} ions in the solutions were reduced to Ag nanocrystals. This is further important quantitative evidence for the redox sorption mechanism of Ag^{I} ions onto the nanograins. Facile collection of silver nanocrystals benefits from the rough and porous structure of the nanograins that is responsible for the superstrong Ag^{I} adsorbability.

Evidence from thermogravimetry: Figure 11 shows the thermogravimetry (TG) and differential thermogravimetry (DTG) curves of 50 mg AN/SA (50/50) copolymer nanograins that have adsorbed Ag^{I} ions. A three-step weight loss process occurs during the thermal decomposition of the Ag-loaded nanograins. The first weight-loss step around 92 °C corresponds to evaporation of water with a mass loss of 3.79%. The second weight-loss step around 203 °C is mainly due to thermal elimination of $-OCH_3$ and $-SO_3H$ side groups with a mass loss of 5.29%. The third weight-loss step centered around 572 °C must be attributed to thermooxidative decomposition of the copolymer chains with a mass loss 42.73%. The residual weight at 700 °C is attributable to Ag nanocrystals thermostable up to 900 °C, because metallic silver is gradually oxidized to Ag_2O in air only at temperatures above 900 °C. The Ag^{I} capacity at an initial Ag^{I} con-

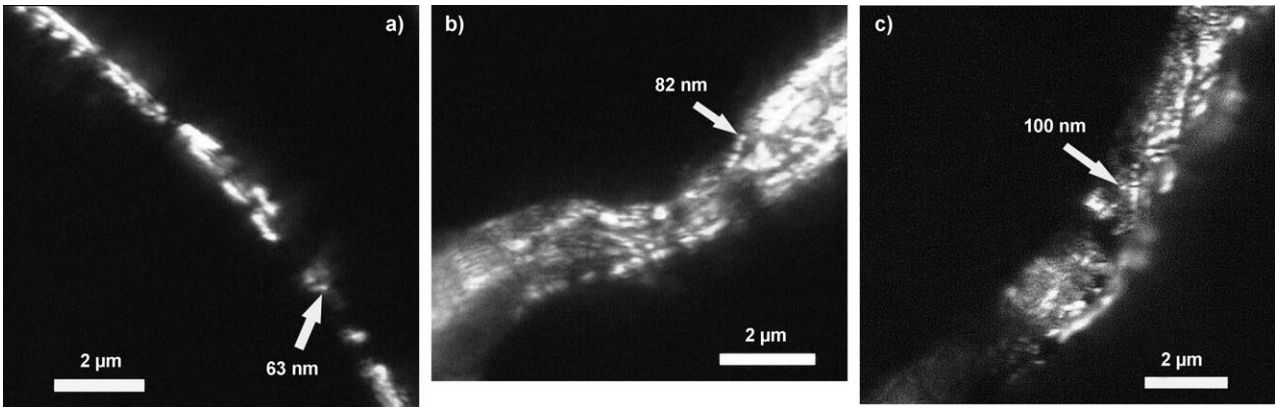

Figure 10. Cross-polarizing micrographs of the Ag nanocrystals in the AN/SA (50/50) copolymer nanograins adsorbing a) 25 mL of 10 mM $AgNO_3$ solution at 30 °C for 0.5 h, b) 25 mL of 10 mM $AgNO_3$ solution at 30 °C for 72 h, and c) practical 19.1 mM Ag^{I} wastewater at 25 °C for 120 h.

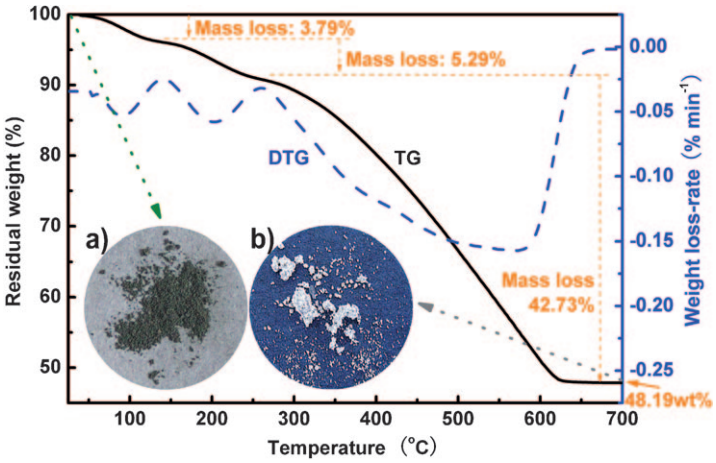

Figure 11. Thermogravimetry and derivative thermogravimetry curves of 50 mg AN/SA (50/50) copolymer particles adsorbing 25 mL 80 mM $AgNO_3$ solution at 30 °C for 120 h. Inset: Images of a) original AN/SA (50/50) copolymer powder adsorbing 25 mL of 80 mM $AgNO_3$ solution at 30 °C for 120 h and b) its cauterant residue at 700 °C in air.

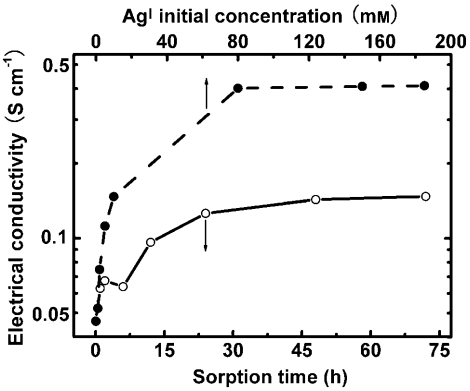

Figure 12. Electrical conductivity variation of AN/SA (50/50) copolymer nanograins with sorption time in 25 mL of 10 mM $AgNO_3$ solution and with initial Ag^{I} concentration in 25 mL of $AgNO_3$ solution for equilibrium sorption time at a fixed sorption temperature of 30 °C.

centration of 80 mM of 1256 mg g^{-1} in Figure 4 implies that the Ag content of 50 mg of Ag-loaded copolymer particles is 50.33 wt %, which is only slightly higher than the residual weight of 48.19 %. It can be speculated that a volatilizable Ag component of 50.33−48.19 = 2.14 % may partly result from a chelation between Ag^{I} and the copolymer. As shown in Figure 11 (inset b), the cauterant residue at 700 °C in air is a spongy, gray, and metallically lustrous substance that should be elemental silver, and is completely different from the dark green Ag-loaded copolymer nanograins (Figure 11, inset a) and black original copolymer nanograins.

Evidence from electrical conductivity of the Ag-loaded nanograins: Based on the four types of structural evidence above, it is certain that the structural changes of the AN/SA copolymers occurred on Ag^{I} sorption. Thus, their physical properties must gradually change during the sorption process. Enhanced electrical conductivity of the copolymer nanograins can also be used to confirm formation of metallic silver during Ag^{I} sorption, because of the doping effect of the highly electrically conducting Ag nanocrystals. Figure 12 shows that the conductivity of the copolymer nanograins adsorbing Ag^{I} gradually rises with increasing Ag^{I} concentration or sorption time, because formation of fine Ag crystal nuclei and then steady Ag crystal growth contribute to improving electrical conductivity until saturation aggregation of Ag crystals on the copolymer chains is reached. When the initial Ag^{I} concentration exceeds 80 mM, the electrical conductivity has an almost constant value of 0.41 S cm^{-1}, that is, nearly ten times higher than that of the original copolymer particles without adsorption of Ag^{I} ions. The slightly reduced conductivity at a sorption time of 6 h can be ascribed to atactic aggregation of Ag crystals.[23] Table 3 shows that the copolymer nanograins adsorbing 200 mg L^{-1} Ag^{I} and 200 mg L^{-1} Hg^{II} display 5.5 times higher conductivity than those only adsorbing 200 mg L^{-1} Ag^{I}. Moreover, the nanograins adsorbing 200 mg L^{-1} Ag^{I} and 400 mg L^{-1} Hg^{II} display 29.7-fold enhancement in conductivity compared with those only adsorbing 200 mg L^{-1} Ag^{I}. This further increased conductivity with Hg^{II} sorption should be assigned to the formation and doping effect of highly conducting arquerite in the copolymer nanograins, whereby the arquerite may originate from an interaction between Ag nanocrystals and liquid elemental mercury, both generated through reduction by the copolymer nanograins, because $AgNO_3$ and $Hg(NO_3)_2$ crystals are not electrically conducting. In conclusion, organic and inorganic hybrid nanocomposites with a widely variable conductivity have been simply fabricated by a sorption technique.

Graphic illustration of the Ag^{I} sorption mechanism: According to the above evidence, four types of sorption mechanisms coexist in the sorption process of Ag^{I} ions onto the AN/SA copolymer nanograins, as summarized in Scheme 1. In the initial period, physical surface sorption, ion-exchange sorption, and chelation sorption successively occur very quickly, and then most of the adsorbed Ag^{I} ions on the nanograins are reduced to elemental Ag at the end of the sorption equilibrium. In other words, reductive sorption of Ag^{I} onto the copolymer is the major mechanism, and the other three kinds of sorption are minor mechanisms.[21]

Reduction of Ag^{I} to Ag^{0} by the AN/SA copolymer after sorption implies that the copolymer acts as a reductant and Ag^{I} as an oxidant. Thus, for a fixed ammonium persulfate oxidant/comonomer molar ratio of 1/1, the copolymer prepared by chemical oxidation of comonomers containing $-NH_2$ but no $-NH-$ groups has a large amount of $-NH-$ groups and a small amount of $-NH_2$ end groups and hence is a proper solid reductant with respect to Ag^{I} ions. Clearly, the as-synthesized copolymer is partly oxidized rather than fully oxidized, as shown in Scheme 1, and the AN/SA copolymer particles are an advanced sorbent for cost-effective recovery of silver nanocrystals directly from various types of Ag^{I} solutions.

Ag^I recovery from practical wastewater by copolymer nanograins: The large amount of silver halide used in the photography industry every year to make photographic film photosensitive unavoidably leads to a huge amount of wastewater containing Ag^I ions in the form of $Ag(S_2O_3)_2^{3-}$, $Ag_2(S_2O_3)_3^{4-}$, and $Ag_3(S_2O_3)_4^{5-}$ in a concentration range usually between 500 and 9000 mg L^{-1}. Since the concentration of residual silver ions in fixing-bath wastewater is quite high, wastewater disposal and silver recovery are important topics. We tested the potential of copolymer nanograins for recovery of silver from wastewater by treating a genuine fixing-bath wastewater sample with AN/SA (50/50) copolymer nanograins for 5 d at room temperature (Table 5).

The adsorptivity and sorption capacity of Ag^I from this wastewater can reach up to 91.9% and 947 mg g^{-1}, respectively, which are much higher than those of 84.5% and 600 mg g^{-1} for Ag^I from $AgNO_3$ at a similar Ag^I concentration (Figure 4), possibly due to different counteranions. Thus, the counteranions influence Ag^I sorption onto the sorbents to some extent. It can be concluded from Figure 4 that the second adsorptivity of Ag^I would be greater than 99.98% if the residual wastewater after the first sorption were retreated with a further 50 mg of nanosorbent. Other metal ions are simultaneously adsorbed by the AN/SA copolymer, but these lighter metal ions coexisting in the fixing bath basically did not influence the Ag^I sorption, consistent with the above results on the effect of coexisting ions in Ag^I solution. Excellent adsorbability of the copolymer nanograins towards Ag^I ions coexisting with other metal ions in the wastewater is thus confirmed.

The form of the adsorbed Ag^I ions on the copolymer sorbent was analyzed by wide-angle X-ray diffraction and cross polarizing microscopy. The three characteristic diffraction peaks of Ag crystal appeared exactly at Bragg angles of 38.1, 44.6, and 64.7°, as in Figure 9. The bright points from anisotropically ordered Ag crystals in cross-polarizing dark field in Figure 10 are another evidence for the formation of fine Ag nanocrystals and their thin aggregation. In short, the sorption process is accompanied by formation of a large number of fine Ag nanocrystals.

The final step of this recovery experiment was to quantitatively isolate the Ag nanocrystals by centrifugation. About 46.98 mg of Ag nanocrystals were obtained at the bottom of the centrifugal tube,[20,31,32] consistent with the 47.35 mg calculated from the sorption capacity. The small discrepancy may be due to experimental error during the extraction process, or to a small amount of Ag^I existing as a chelate on the copolymer chains. Regardless, a large amount of silver was recovered from the wastewater by the copolymer nanosorbents, that is, both purification and recovery of precious silver from wastewater are accomplished at the same time. Moderate adsorptivity for another four coexisting ions, namely, $Fe^{III\&II}$, Na^I, Al^{III}, and K^I, was observed (Table 5). Fortunately, their interaction with the copolymer nanoparticles occurs mainly by complexation, and it seems that these complexes did not interfere with the centrifugal separation and recovery of the much heavier silver crystals from the much lighter nanoparticles and their complexes with the four coexisting ions. In short, the copolymer nanograins have simply been used to turn environmental trash into treasure.

Conclusion

High-performance AN/SA (50/50) copolymer nanograins synthesized by facile chemical oxidative copolymerization exhibit the highest Ag^I sorption capacity so far of up to 2034 mg g^{-1} (18.86 mmol g^{-1}) and accomplish nearly 100% Ag^I adsorption from dilute solution. The effects of five crucial parameters, namely AN/SA ratio, initial Ag^I concentration, sorption time, ultrasonic treatment, and coexisting ions, on Ag^I sorption were systematically optimized. The sorption mechanism of Ag^I onto the copolymer nanograins was explored by eight analytical methods, which revealed that a redox interaction between Ag^I ions and the copolymer nanograins is the most important sorption mechanism, because almost all adsorbed Ag^I ions on the nanograins were reduced in situ to fine Ag nanocrystals. The AN/SA copolymer nanograins show effective recovery of Ag^I ions from genuine wastewater that even contains various other metal ions like Hg^{II}, Pb^{II}, Cu^{II}, Fe^{III}, Al^{III}, K^I, and Na^I, and thus turn trash into treasure. The experimental Ag^I sorption capacity of 18.86 mmol g^{-1} is much higher than the experimental Hg-ion sorption capacity of 10.28 mmol g^{-1} onto the same nanosorbents.[21] In other words, the AN/SA (50/50) copolymer nanograins are very strong Hg-ion nanosorbents and ultrastrong Ag^I nanosorbents. At the same time, a unique hybrid Ag nanocrystal/copolymer nanograin nanocomposite with widely controllable electrical conductivity and potential application as electrode modifier due to its high catalytic activity[7] was facilely obtained as the result of Ag^I sorption. To sum up, the AN/SA (50/50) copolymer nanograins carrying numerous functional groups on their porous and rough structure are not only outstanding Ag^I sorbents with a bright future for removal and recovery of noble Ag^I from typical wastewaters, but also novel multifunctional materials having excellent redox reactivity, intrinsic electrical conductivity, high environmental stability, and practical recoverability of Ag as Ag nanocrystals.

Experimental Section

Chemical reagents: Aniline (AN), 5-sulfo-2-methoxyaniline (SA), ammonium persulfate, $AgNO_3$, $Hg(NO_3)_2$, $Pb(NO_3)_2$, $Cu(NO_3)_2$, and $BaCl_2$ of analytical-reagent grade were commercially obtained and used as received.

Synthesis of AN/SA copolymer nanograins:[21] Copolymer nanoparticles with five AN/SA molar ratios were prepared by simple chemical oxidative polymerization. A typical preparation procedure of the AN/SA (50/50) copolymer nanograins is as follows: AN monomer (2.275 mL, 25 mmol) and SA monomer (5.075 g, 25 mmol) were added to HCl (1.0 M, 150 mL) at 25 °C in a 250 mL glass flask. Ammonium persulfate (11.4 g, 50 mmol) was dissolved individually in HCl (1.0 M, 50 mL) to give an oxidant solution, which was dropped into the mixed comonomer solution at a rate of one drop (ca. 60 μL) every 3 s at 25 °C to give a final co-

monomer/oxidant molar ratio of 1/1. The reaction mixture was vigorously magnetically stirred for 24 h at 25 °C. The resulting copolymer nanograins were washed thoroughly with distilled water by centrifugation to remove the residual oxidant, water-soluble oligomers, and byproducts until no SO_4^{2-} was evident on dripping $BaCl_2$ solution into the filtrate. The solid black particles were left to dry in ambient air at 40 °C for 7 d. The nominal polymerization process is shown in Scheme 1:

Sorption of Ag^I onto AN/SA copolymer nanograins: Sorption of Ag^I on the AN/SA copolymer nanograins in aqueous solution was performed in a batch experiment. An aqueous $AgNO_3$ solution (25 mL) with Ag^I concentration ranging from 1 to 200 mM was adsorbed on a given amount of the particles at a fixed temperature of 30 °C. After a certain sorption time, the particles were filtered from the solution, and then the Ag^I concentration in the filtrate was measured by Volhard titration at higher Ag^I concentration or inductively coupled plasma (ICP) at lower Ag^I concentration. The adsorbed amount of Ag^I on the particles was calculated according to an earlier report.[21]

Preparation of copolymer sample for cross-polarizing microscopy observation: After the sorption process, the Ag-loaded AN/SA copolymer particles were left to dry in ambient air at room temperature, and then 1 mg solid particles were placed in a beaker and soaked in 50 mL deionized water for several days. Before cross-polarizing microscopic observation, the particles were ultrasonically treated at 40 kHz for 15 min in a DL-180A ultrasonic machine made in China to make sure that the solid particles were evenly dispersed. A drop of the dispersion was dropped onto a piece of clean slide glass, and then the slide glass was covered with a cover glass slowly and carefully to avoid generation of bubbles.

Preparation of solution with coexisting ions: The effect of coexisting ions on Ag^I adsorbability onto the AN/SA copolymer nanosorbents was investigated to disclose possible interaction with and sorption selectivity of Ag^I over other heavy-metal ions such as Hg^{II}, Pb^{II}, and Cu^{II}. Mixed solutions of the metal ions were prepared by dissolution of $AgNO_3$, $Hg(NO_3)_2$, $Pb(NO_3)_2$, and $Cu(NO_3)_2$ in deionized water. In the Ag^I/Hg^{II} system, the initial Ag^I and Hg^{II} concentrations are fixed at 200/0, 200/200, 200/400 mg L^{-1}. In the $Ag^I/Pb^{II}/Cu^{II}$ system, the initial $Ag^I/Pb^{II}/Cu^{II}$ ion concentrations were 50/50/50 mg L^{-1}.

Practical Ag^I wastewater sample: A genuine Ag^I wastewater sample was obtained from a Kodak Photo Gallery in Shanghai, China. The fixing bath used in this gallery, made in Tianjin, China has 50 wt% $Na_2S_2O_3$ and 25 wt% EDTA ferric ammonium as main ingredients. This practical wastewater sample contains mainly Ag^I, Fe^{III}, Fe^{II}, Na^I, Al^{III}, and K^I ions in concentrations of 2.06, 3.09, 1.97, 0.014, and 0.65 g L^{-1}, respectively, according to ICP testing. The initial pH of the wastewater was 5.5, measured with a pHS-3C digital display acidometer.

Measurements: The IR spectra were recorded on Bruker Equinox 55 (Germany)/Hyperion 2000 FT-IR spectrometer with a resolution of $<0.5\ cm^{-1}$, a wavenumber precision of better than $0.01\ cm^{-1}$, and a signal/noise ratio of >3600:1 by the ATR method. UV/Vis spectra of the copolymers in DMSO were obtained on a Perkin-Elmer Instruments Lambda 35 at a scanning rate of 480 nm min^{-1}. Wide-angle X-ray diffraction was performed on a D/max 2550 VB3 X-ray diffraction analyzer with $Cu_{K\alpha}$ radiation at a scanning rate of 5° min^{-1}. The particle samples for field-emission scanning electron microscopy (SEM, Philips XL30 FEG) were dispersed on glass and subjected to gold sputtering prior to observation. The size of the particles in water was analyzed with an LS230 laser particle-size analyzer from Beckman Coulter, Inc. The fine silver microcrystals were observed under a Leica XS-402P polarizing microscope made in Germany. Nitrogen adsorption/desorption isotherms were measured with a Micromeritics Tristar 3000 analyzer at 77 K. The BET method was utilized to calculate the surface area. The pore volume and pore size distributions were derived from the adsorption branches of the isotherms by the BJH method. The pH value of the adsorption solution was measured by a PHS-3C pH digital indicator. Thermogravimetry was carried out at a heating rate of 10 °C min^{-1} within the temperature range of 30–700 °C with a Stanton-Redcroft STA 449 C Jupiter TG analyzer in static air atmosphere. The relative error for the various measurements is less than 5%.

Acknowledgements

The project is supported by the National Natural Science Foundation of China (20974080) and the Foundation of Key Laboratory of Molecular Engineering of Polymers, Fudan University, China. We would like to thank Prof. Dr. Qiu-Feng Lü for her important help.

[1] a) M. Liong, B. France, K. A. Bradley, J. I. Zink, *Adv. Mater.* **2009**, *21*, 1684–1689; b) J. Thiel, L. Pakstis, S. Buzby, M. Raffi, C. Ni, D. J. Pochan, S. I. Shah, *Small* **2007**, *3*, 799–803.
[2] F. Xu, C. Dong, C. Xie, J. Ren, *Chem. Eur. J.* **2010**, *16*, 1010–1016.
[3] K. Matsubara, T. Tatsuma, *Adv. Mater.* **2007**, *19*, 2802–2806.
[4] A. Laguna, T. Lasanta, J. M. Lopez-de-Luzuriaga, M. Monge, P. Naumov, M. E. Olmos, *J. Am. Chem. Soc.* **2010**, *132*, 456–457.
[5] L. Maretti, P. S. Billone, Y. Liu, J. C. Scaiano, *J. Am. Chem. Soc.* **2009**, *131*, 13972–13980.
[6] R. Klajn, P. J. Wesson, K. J. M. Bishop, B. A. Grzybowski, *Angew. Chem.* **2009**, *121*, 7169–7173; *Angew. Chem. Int. Ed.* **2009**, *48*, 7035–7039.
[7] N. C. Bigall, A.-K. Herrmann, M. Vogel, M. Rose, P. Simon, W. Carrillo-Cabrera, D. Dorfs, S. Kaskel, N. Gaponik, A. Eychmuller, *Angew. Chem.* **2009**, *121*, 9911–9915; *Angew. Chem. Int. Ed.* **2009**, *48*, 9731–9734.
[8] P. Barbaro, F. Liguori, *Chem. Rev.* **2009**, *109*, 515–529.
[9] Y.-L. Lam, D. Yang, C.-Y. Chan, K.-Y. Chan, P. H. Toy, *Ind. Eng. Chem. Res.* **2009**, *48*, 4975–4979.
[10] A. A. Atia, *Hydrometallurgy* **2005**, *80*, 98–106.
[11] Z. R. Yue, W. Jiang, L. Wang, H. Toghiani, S. D. Gardner, C. U. Pittman, *Carbon* **1999**, *37*, 1607–1618.
[12] Y. Kanai, T. Oshima, Y. Baba, *Ind. Eng. Chem. Res.* **2008**, *47*, 3114–3120.
[13] M. Cox, A. A. Pichugin, E. I. El-Shafey, Q. Appleton, *Hydrometallurgy* **2005**, *78*, 137–144.
[14] J. Hanzlık, J. Jehlicka, O. Sebek, Z. Weishauptova, V. Machovic, *Water Res.* **2004**, *38*, 2178–2184.
[15] Z. J. Yu, A. N. Zhou, J. L. Qu, T. J. Zhang, *Microporous Mesoporous Mater.* **2005**, *85*, 104–110.
[16] M. J. Manos, M. G. Kanatzidis, *Chem. Eur. J.* **2009**, *15*, 4779–4784.
[17] X. G. Li, M. R. Huang. W. Duan, Y. L. Yang, *Chem. Rev.* **2002**, *102*, 2925–3030.
[18] A. G. MacDiarmid, *Angew. Chem.* **2001**, *113*, 2649–2659; *Angew. Chem. Int. Ed.* **2001**, *40*, 2581–2590.
[19] A. O. Patil, A. J. Heeger, F. Wudl, *Chem. Rev.* **1988**, *88*, 183–200.
[20] X. G. Li, X. L. Ma, J. Sun, M. R. Huang, *Langmuir* **2009**, *25*, 1675–1684.
[21] X. G. Li, H. Feng, M. R. Huang, *Chem. Eur. J.* **2009**, *15*, 4573–4581.
[22] X. G. Li, M. R. Huang, S. X. Li, *Acta Mater.* **2004**, *52*, 5363–5374.
[23] X. G. Li, R. Liu, M. R. Huang, *Chem. Mater.* **2005**, *17*, 5411–5419.
[24] Z. N. Shu, C. H. Xiong, X. Wang, *Trans. Nonferrous Met. Soc. China* **2006**, *16*, 700–704.
[25] C. Chen, J. L. Wang, *J. Hazard. Mater.* **2008**, *151*, 65–70.
[26] Z. Aksu, *Sep. Purif. Technol.* **2001**, *21*, 285–294.
[27] B. J. Palys, M. Skompska, K. Jackowska, *J. Electroanal. Chem.* **1997**, *433*, 41–48.
[28] C. Dearmitt, C. P. Armes, J. Winter, *Polymer* **1993**, *34*, 158–162.
[29] W. M. De Azevedo, I. L. Mattos, M. Navarro, E. F. Silva, *Appl. Surf. Sci.* **2008**, *255*, 770–774.
[30] J. H. Kim, C. K. Kim, J. Won, Y. S. Kang, *J. Membr. Sci.* **2005**, *250*, 207–214.
[31] R. Sanghi, P. Verma, *Bioresour. Technol.* **2009**, *100*, 501–504.
[32] N. S. Shaligram, M. Bule, R. Bhambure, R. S. Singhal, S. K. Singh, G. Szakacs, A. Pandey, *Process Biochem.* **2009**, *44*, 939–943.

Received: February 26, 2010
Revised: May 9, 2010
Published online: July 19, 2010

